Received: 13 May 2022 | Revised: 13 September 2022 | Accepted: 16 September 2022

DOI: 10.1111/mec.16701

ORIGINAL ARTICLE

MOLECULAR ECOLOGY WILEY

Linking pathogen–microbiome–host interactions to explain amphibian population dynamics

María Torres-Sánchez | Ana V. Longo

Department of Biology, University of Florida, Gainesville, Florida, USA

Correspondence
María Torres-Sánchez, Department of Biology, University of Florida, Gainesville, Florida, USA.
Email: torressanchez.maria@gmail.com

Funding information
National Science Foundation, Grant/Award Number: IOS-1310036 and IOS-2011278

Handling Editor: Kayla King

Abstract

Symbiotic interactions can determine the evolutionary trajectories of host species, influencing genetic variation through selection and changes in demography. In the context of strong selective pressures such as those imposed by infectious diseases, symbionts providing defences could contribute to increase host fitness upon pathogen emergence. Here, we generated genome-wide data of an amphibian species to find evidence of evolutionary pressures driven by two skin symbionts: a batrachochytrid fungal pathogen and an antifungal bacterium. Using demographic modelling, we found evidence of decreased effective population size, probably due to pathogen infections. Additionally, we investigated host genetic associations with infection status, antifungal bacterium abundance and overall microbiome diversity using structural equation models. We uncovered relatively lower nucleotide diversity in infected frogs and potential heterozygote advantage to recruit the candidate beneficial symbiont and fight infections. Our models indicate that environmental conditions have indirect effects on symbiont abundance through both host body traits and microbiome diversity. Likewise, we uncovered a potential offsetting effect among host heterozygosity–fitness correlations, plausibly pointing to different ecological and evolutionary processes among the three species due to dynamic interactions. Our findings revealed that evolutionary pressures not only arise from the pathogen but also from the candidate beneficial symbiont, and both interactions shape the genetics of the host. Our results advance knowledge about multipartite symbiotic relationships and provide a framework to model ecological and evolutionary dynamics in wild populations. Finally, our study approach can be applied to inform conservation actions such as bioaugmentation strategies for other imperilled amphibians affected by infectious diseases.

KEYWORDS
Acinetobacter rhizosphaerae, *Batrachochytrium dendrobatidis*, co-evolution, *Eleutherodactylus coqui*, heterozygosity–fitness correlations, host genetic variation, symbiosis

1 | INTRODUCTION

Symbiosis, defined as living together in physical contact between different species, greatly impacts many aspects of organismal biology. The pervasiveness of these systems in nature led Lynn Margulis to propose that symbiotic interactions are one of the major drivers of evolution (Margulis, 1998). Many characteristics of these associations can vary, including direction of cost/benefit effects, degree of dependence between partners and symbiont transmission traits. This variation profoundly affects ecological and evolutionary

processes (Fisher et al., 2017; Hayward et al., 2021; Hurst, 2017; McFall-Ngai et al., 2013). While some hosts and mutualists commonly show strong patterns of co-adaptation and co-diversification (e.g., endosymbionts with vertical transmission), hosts and their parasites present more disparate evolutionary trajectories characterized by phylogenetic incongruencies (Hayward et al., 2021). In the case of parasitism, negative interactions impose selective forces in host evolution, leaving genomic footprints and creating genetic susceptibility landscapes (Weatherall et al., 1997). The relationships can be extremely complex, as parasites co-evolve with their hosts, cascading effects can alter previously established interactions and these symbionts (e.g., defensive symbionts) in turn can reshape parasite–host interplay (Hopkins et al., 2017; Vorburger & Perlman, 2018). A better understanding of these multipartite relationships will advance our knowledge and predictions about co-evolutionary dynamics, ultimately improving disease control and mitigation strategies in wildlife conservation (DeCandia et al., 2018).

One group of organisms that exhibits a wide variety of symbiotic associations is fungi (Naranjo-Ortiz & Gabaldón, 2019a, 2019b). Fungal symbionts can perform different roles from essential mutualists, such as mycorrhizal fungi (van der Heijden et al., 2015), to master parasites, for example the ant-infecting *Ophiocordyceps* (Andersen et al., 2009), or pathogens able to cause devastating infectious diseases (Fisher et al., 2020, 2012). Human activities have contributed to the spread of this group of organisms, and pathogenic fungi pose an important threat to biodiversity (Fisher et al., 2020). For instance, the infectious disease chytridiomycosis, caused by the skin-infecting fungus *Batrachochytrium dendrobatidis* or *Bd* (Longcore et al., 1999), has contributed to population declines, extirpations and extinctions of many amphibian species worldwide, being considered the utmost disease-driven loss of wildlife ever recorded (Fisher & Garner, 2020). It is now increasingly rare to find regions where amphibian communities are *Bd*-free (Olson et al., 2021). Hence, amphibian populations are plausibly in arms race dynamics evolving defence systems to persist by limiting the negative consequences of infection. Selection in components of the major histocompatibility complex (MHC) has been documented for populations of many amphibian species under differing disease regimes (Belasen et al., 2022; Fu & Waldman, 2017; Kosch et al., 2016; Savage & Zamudio, 2011). The risk for new outbreaks after pathogen emergence is context-dependent following the conceptualized model known as the disease triangle: host–pathogen–environment (Scholthof, 2007). Enzootic rather than epizootic scenarios are commonly now being documented, noting the importance of host immunity and amphibian skin microbiome to the disease outcome (Bates et al., 2018; Briggs et al., 2010; Jani et al., 2017). After the discovery of multiple amphibian skin bacterial taxa with *Bd* inhibitory activity (Woodhams et al., 2015), chytridiomycosis research efforts have focused largely on describing protective microbes and analysing interspecific differences in skin microbiome diversity and structure. Whereas *Bd*–host and *Bd*–microbiome studies have provided insights into infections dynamics (Brannelly et al., 2021), the multipartite pathogen–microbiome–host interaction remains unexplored to a great extent, specifically its co-evolution and the study of the selective forces that both symbionts exert on their hosts and between each other.

Among the amphibian species under an enzootic disease regime with variable response to *Bd* infection outbreak is the common coqui (*Eleutherodactylus coqui* Thomas, 1966), a frog endemic to Puerto Rico. This direct-developing frog exhibits infection cycles modulated by different factors including seasonal environmental conditions, ontogenetic stage, microhabitat use and skin microbial community (Burrowes et al., 2017; Langhammer et al., 2014; Longo et al., 2010; Longo & Zamudio, 2017). During the warm-wet season, frogs withstand *Bd* infection, whereas a high percentage of *Bd*-infected frogs (50%–60%) die during the cool-dry season with acute *Bd* infections (Longo et al., 2010). Frogs at the early stages of their life have lower survival rates when infected (Langhammer et al., 2014). Likewise, frogs found in bromeliads or on the forest floor carry higher infection intensities than active frogs in high branches or tree trunks (Burrowes et al., 2017). Over the environmental conditions that provide a survival advantage to the hosts, frogs may recruit candidate beneficial bacteria such as *Acinetobacter rhizosphaerae* to fight infection (Longo & Zamudio, 2017). Several isolates of this bacterial taxon from different amphibian hosts occurring in many regions of the world inhibited *Bd* growth during culture assays (Woodhams et al., 2015). Together, this variation points to the potential co-evolution and adaptation of coquí frogs to coexist with this pathogen, which was detected for the first time in El Yunque National Forest, Puerto Rico, in a frog collected in 1976 (Burrowes et al., 2004).

In this study, we examined three-species interactions: *Bd*, *A. rhizosphaerae*, and *E. coqui* to assess role of symbionts in host evolution (Figure 1). We characterized the genetic variation of a coquí population consisting of frogs under different infection statuses to uncover evidence of selection related to *Bd*. We also investigated population admixture and demographic history to determine the extent of disease-driven declines in the genetic diversity of this frog population. Finally, we defined a statistical framework to test frog heterozygosity–fitness correlations among infection status, candidate protective microbe abundance and skin microbiome diversity metrics. Our study contributes to the establishment of groundwork to interrogate pathogen–microbiome–host interactions not only in amphibians under enzootic chytridiomycosis, but also in different symbiotic systems with multipartite relationships affecting species ecology and evolution.

2 | MATERIALS AND METHODS

2.1 | Experiment, samples and genomic data set

We selected as a model system the common coqui frog from Palo Colorado Forest at El Yunque. These frogs were part of a mesocosm experiment to test the effect of seasonality and skin microbiome on the *Bd* infection outcome (Longo & Zamudio, 2017). Animals were randomly assigned to the different experimental categories (i.e., dry

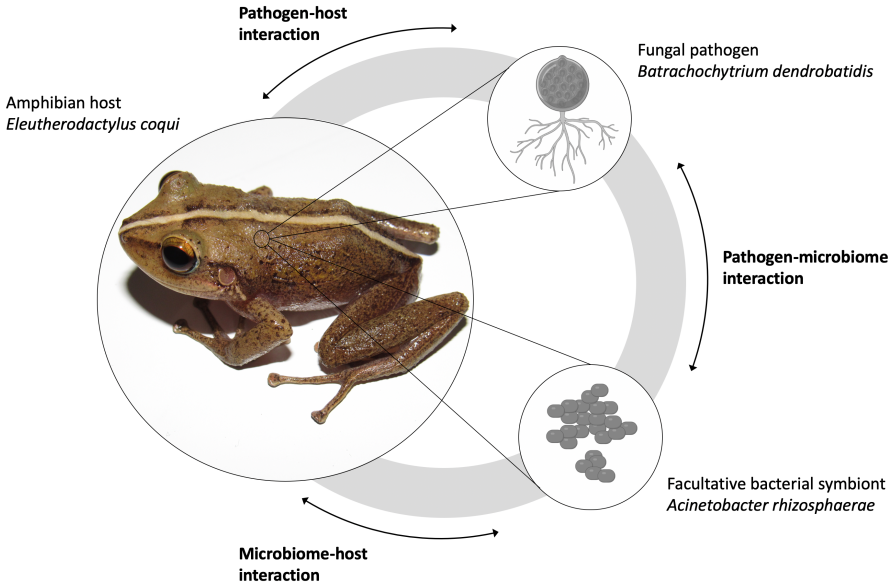

FIGURE 1 The multipartite pathogen–microbiome–host interactions. The trifecta of this study is represented by a picture of a coqui frog (photo authorship M.T.-S.) and icons of a chytrid fungal zoosporangium and coccobacilli (icons source BioRender) [Colour figure can be viewed at wileyonlinelibrary.com]

and wet season, inoculation of 10^6 *Bd* JEL427 zoospores [Bd+] and controls [Bd−], reduction of skin microbiome by applying 1.5% hydrogen peroxide [HP+] and controls [HP−]; for more information about the experimental design see Longo & Zamudio, 2017) and maintained in field enclosures for 15 days. Frog measurements (weight and snout–vent length [SVL]) and skin swab samples for both quantifying *Bd* infection intensity and characterizing the skin microbiome were taken initially (day 0) and every 3 days during the experiment (data time points: 3, 6, 9, 12 and 15 days). The pathogen load was measured as *Bd* gene fragment equivalents from quantitative polymerase chain reaction (qPCR) assays. Skin microbiome community metrics (number of observed operational taxonomic units [OTUs], phylogenetic distances, Shannon index and Dominance index) were obtained from 16S rRNA amplicon sequencing data using the QIIME pipeline (Caporaso et al., 2010). For a detailed explanation regarding the methods of *Bd* quantification and the microbiome data see Longo and Zamudio (2017). Swab data were obtained for the frogs initially (upon capture) and during the experiment while documenting animal infection recovery. These data (frog weight, frog SVL, *Bd* quantification, number of skin microbiome OTUs, skin microbiome Shannon index, skin microbiome Dominance index, skin microbiome phylogenetic distances and candidate antifungal bacterium sequencing counts; see Appendix S1) were available from the supplementary materials of the previously published study (Longo & Zamudio, 2017).

After the experiment, we extracted DNA from the liver of euthanized frogs using the QIAGEN DNeasy Blood and Tissue kit. A total of 77 adult frogs were selected based on DNA quality and quantity and completeness of both the skin microbiome and the *Bd* infection data previously published (Longo & Zamudio, 2017). We sent DNA aliquots to the Cornell Institute for Genomic Diversity to perform genotyping by sequencing (GBS; Elshire et al., 2011), which were digested using the methylation-sensitive restriction enzyme *Eco*T22I (recognition sequence: ATGCAT, that might be affected by ATG5mCAT and ATGC6mAT). We sequenced the samples using a single-end 100-bp Illumina HiSeq 2000 lane. The raw sequence reads, which comprised almost 250 million reads (247,949,836), were converted into tag-SNP (single nucleotide polymorphism) genotypes by using the UNEAK pipeline with default parameters as implemented in TASSEL 5.0 (Bradbury et al., 2007; Glaubitz et al., 2014). Filters were applied to discard monomorphic loci, which could be potentially paralogues, by removing any locus with a mean observed heterozygosity <0.05 or >0.75. In the final variant calling file (vcf, initial genomic data set or data set 1, see Appendix S2), only polymorphic loci with <10% of missing genotypes across all the individuals were considered to avoid technical and/or biological biases (e.g., different methylation patterns per frog). To demonstrate the stringency of our variant filtration method, we simulated *Eco*T22I digestion and predict the number of expected loci for the common coqui frog genome assembly (GCA_019857665.1) using SIMRAD (Lepais & Weir, 2014).

2.2 | Calculating genomic diversity

We converted the initial genomic data set to flat files (map/ped) using VCFTOOLS 0.1.13 (Danecek et al., 2011) and, subsequently, to binary file (bed) and its associated files (bim/fam) using PLINK 1.90b6.15 (Purcell et al., 2007). We computed several statistics and metrics using the aforementioned programs to characterize the genomic data set and also as a quality control procedure. We calculated missing rates, both missingness by variant position and by frog specimen, using the --missing PLINK option. We created five data sets by filtering variants out and increasing the genotyping rate from 0.95 to 1 (see Table S1 for detailed information about the filtered data sets). Because downstream results may vary based on filtering processes (Schmidt et al., 2021), we performed analyses for all data sets (initial genomic data set: defined as *data set 1*; and filtered data sets with increased genotyping rate: *data sets 2 to 5*) to evaluate the effect of missing variants. For frog-based statistics, we computed inbreeding coefficient, *F*, and heterozygosity ratios (heterozygous/homozygous

ratio) using the --het parameter of VCFTOOLS and vcfstats of RTG TOOLS (https://github.com/RealTimeGenomics/rtg-tools), respectively. We estimated and plotted the conditional densities of the frog infection status over frog multilocus heterozygosity using R (R Core Team, 2019). We performed subsequent genetic analyses in duplicate using *data set 1* (genotyping rate 0.95) and *data set 5* (genotyping rate 1).

For variant-based statistics within the frog samples, we estimated allelic frequencies using the --freq PLINK option and tested deviation from Hardy–Weinberg equilibrium (HWE, deviated variants $p < .05$) using the --hardy PLINK option. To identify candidate variants that do not fit the neutral theory model (Tajima, 1989), we computed Tajima's D using the --TajimaD VCFTOOLS option. We calculated nucleotide diversity from average pairwise differences between all frog pairs using the --site-pi VCFTOOLS option. We compared these variant metrics for *data sets 1* and *5* grouping separately initially *Bd*-infected and uninfected individuals (43 and 34 frogs, respectively) and selecting variants that deviate from HWE with loss of heterozygosity (deviated variants with gain of heterozygosity were considered as genotyping errors). We visualized the genetic metrics and tested equality of Tajima's D values between *Bd*-infected and uninfected using a Mann–Whitney–Wilcoxon test with R (R Core Team, 2019).

2.3 | Population structure, molecular variance and demographic analyses

To study relationships among the 77 coqui frogs, we used multidimensional scaling (MDS) analysis with 10 dimensions on a computed pairwise genetic distances matrix of identity by state (IBS), and estimated kinship coefficients using --cluster --mds-plot PLINK options (Purcell et al., 2007), and --relatedness2 VCFTOOLS option (Danecek et al., 2011), respectively. We visualized the genetic distances clustered by MDS dimensions in scatter plots and represented pairwise kinship coefficients as an estimation of identity by descendent (IBD) matrix on a heatmap using R (R Core Team, 2019). We also used the distance matrix obtained through the --distance square 1-ibs PLINK option to analyse the molecular variance partitioning the samples by initial infection status with the function AMOVA of the R package PEGAS (Paradis, 2010). To further explore population stratification, we estimated individual ancestries by maximum likelihood searches using ADMIXTURE 1.3.0 (Alexander et al., 2009) with cross-validation procedure, --cv. We used five independent search seeds to find the most likely number of ancestral populations, *K*, testing values from 1 to 10. We performed these population structure and molecular variance analyses for *data set 1* and *5*, and for the same data sets containing only variants that deviate from HWE with loss of heterozygosity. We visualized cross-validation errors and ancestry fractions using scatter and stacked bar plots in R (R Core Team, 2019).

To estimate demographic parameters, we built a folded one-dimension site frequency spectrum (SFS) file using EASYSFS (https://github.com/isaacovercast/easySFS). We computed the folded SFS maximizing the number of samples (77 diploid individuals and 1102 variants). We explored two different evolutionary scenarios or models (equilibrium and bottleneck; Figure 2) using coalescent simulations with FASTSIMCOAL 2.6.0.3 (Excoffier et al., 2013) with a conservative mutation rate of 1e-9 (Crawford, 2003). To fit the two demographic models, we ran both models 100 independent times or runs, each run with one million of coalescent simulations and 100 optimization cycles (ECM). To compare the demographic models, we calculated likelihood distributions and nonparametric bootstraps using the parameter files generated in the run with the smallest difference between the maximum observed likelihood (MaxObsLhood) and the estimated likelihood (MaxEstLhood) under each model.

2.4 | Statistical analyses of symbiotic interactions and disease outcome

To link pathogen–microbiome–host interactions, we performed regression and association analyses. First, we grouped the variables into two trait data sets (*initial* and *experimental* data sets, see

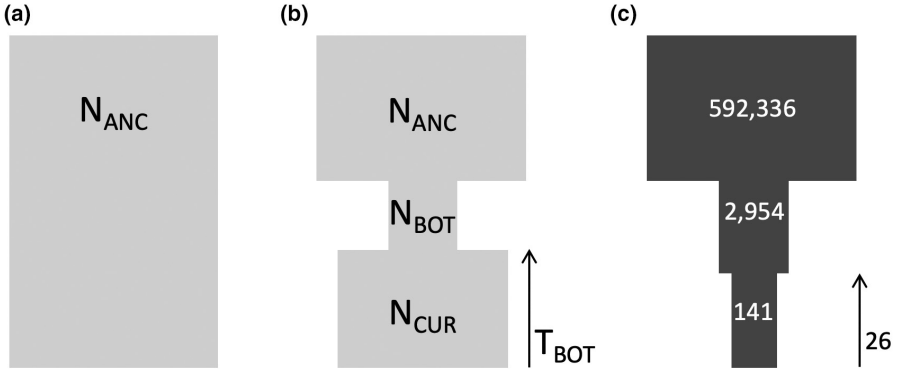

FIGURE 2 Demographic models. Hypothesized theoretical demographic models: Equilibrium (a) and bottleneck (b). Abbreviations represent parameters to infer during the analyses. Equilibrium models test whether population size has been invariant and estimates ancestral population size (N_{ANC}) while bottleneck scenarios test for changes in population effective size and estimate the different sizes during the population fluctuations (N_{ANC}, population size during bottleneck or N_{BOT}, and current population size or N_{CUR}) as well as the time to the bottleneck (T_{BOT}). (c) the demographic model for our coqui population with the estimated parameters

Appendix S1) to disentangle any possible effects due to *Bd* strain interactions (Greenspan et al., 2018). *Initial* values included the data acquired from frogs upon capture, whereas the *experimental* values group responses from days 3 to 15 of the experiment. We explored the distributions of these two trait data sets as well as bivariate relationships, transforming values as required. To reduce the dimensionality of the microbiome data, we combined microbiome metrics previously published by Longo & Zamudio, 2017 (number of observed OTUs, phylogenetic distances, Shannon index and Dominance index), which were highly correlated, by principal components analyses (PCAs) using the R prcomp function with scaling option (R Core Team, 2019). We created a new variable, defined hereafter as *microbiome diversity index*, using the PC1 loadings of which positive values were related to a high number of observed OTUs, phylogenetic distances, and Shannon indexes, whereas negative values were related to high Dominance index (Figure S1). To describe the change of the skin microbiome through the experiment, we computed linear models for each frog using the *microbiome diversity index* as the response variable and data time points as the predictor with the lm function in R (R Core Team, 2019). We visualized the values of the skin microbiome index and its regression lines using R in scatterplots, grouping the data for each frog by experiment category (Bd−, Bd+, HP−, HP+, dry season and wet season; see Figure S2). From the slope estimates (β_1) of these models, we added another new variable, change in microbiome diversity, to the experimental data set. Likewise, we followed the same procedure to describe the change in *Bd* load and the abundances of *A. rhizosphaerae* (sequencing counts of the candidate antifungal bacterium), deriving two variables from the slopes of the linear regressions: change of *Bd* load and change of *A. rhizosphaerae* abundance, respectively (see Figures S3 and S4). We calculated body condition using the residuals of the linear model between frog weight grouped by sex as the response variable and SVL as the predictor using the lm function in R (see Figure S5).

After these analyses and variable transformations, we computed two structural equation models (for the *initial* and the *experimental* data sets) using the psem function of the R package PIECEWISESEM version 2.1.0 (Lefcheck, 2016) to explain endogenous variable variation of: (i) initial *Bd* infection status (modelled as numerical using a binomial distribution since categorical variables were not implemented in PIECEWISESEM), initial *A. rhizosphaerae* abundance (this variable showed skewed distributions, was log-transformed for visual representation in Figure S6, and was modelled using negative binomial distribution), microbiome diversity index (modelled using a gaussian distribution), and frog body condition (modelled using a gaussian distribution) in relation to the exogenous variables: Puerto Rican climatic seasons and frog heterozygosity (values from heterozygous/homozygous ratios of the genomic *data set 1*); and (ii) change in *Bd* (modelled using a gamma distribution), change in *A. rhizosphaerae* (modelled using a gamma distribution), change in microbiome diversity index (modelled using a gaussian distribution), frog condition (modelled using a gaussian distribution), and frog recovery (modelled using a binomial distribution) related to the aforementioned exogenous variables plus treatment variable (see variable exploratory relationships in the Figures S6 and S7, and model equations with complete code for our methodology in Appendix S3). We built path relationships and designed directed acyclic graphs underlying model equations based on both previous information regarding this particular biological system and our hypothesis testing process.

3 | RESULTS

We obtained 8590 tag-SNPs with a proportion of missing loci less that 10% from the 77 coqui frogs. The simulated number of restriction sites was 103,717, which evidenced our stringent filter processes. The highest missingness by locus in the initial genomic data set was 9.091% for a total of 724 variant positions (see Table S1 for information about genotyping rates and SNP numbers). Regarding the proportion of missing information per frog in the initial data set, we found that six individuals presented an SNP missingness proportion higher than 10% (the individual with the highest missingness proportion, 40%, was the frog with the identification code MD030, followed by MD047, MD027, MD022, MW045 and MD037; see Appendix S1). The genotyping rates of the five built data sets are presented in Table S1, and filtering effects between the computed inbreeding coefficient *F* and heterozygosity ratios per frog are shown in Figure S8. In the initial genomic data set, or *data set 1*, these negatively correlated metrics ranged from 0.72 to 0.04 and from 0.57 to 4.38, respectively. Conditional probabilities of the infection status revealed that frogs with low heterozygosity ratios were more likely to be *Bd*-infected (Figure 3). However, we still detected some uninfected individuals with low heterozygous/homozygous ratio (the two frogs with the highest missingness proportion, MD047 and MD030, had a heterozygosity ratio <1; see Appendix S1). Individuals with the highest inbreeding coefficient (lower heterozygosity ratio) were those with highest SNP missingness proportion of all the data sets. These metrics were highly correlated between *data set 1* and the others including *data set 5* (the data set with genotyping rate of 1), showing little effect of the missing loci on the overall metric values per frog (see Figure S9). The strength of the relationship between heterozygosity ratios from *data set 1* and from *data set 5* was the weakest of these linear correlations ($r = .76$; see Figure S9D), and therefore we further explored variant-based statistics of both data sets (*data sets 1 and 5*). A high percentage of variant positions showed a minor allele frequency (MAF) <0.1 (33.52% and 28.86% of *data set 1* and *data set 5*, respectively; see Table S2 and Figure S10 for the MAF distributions plot). Evolutionary forces affect allele frequencies, and in consequence variant positions can deviate from HWE. We found a total of 3806 variants in *data set 1* and 304 in *data set 5* that deviated from HWE. The relationships among the other metrics that pointed to different evolutionary processes (Tajima's D and nucleotide diversity) in relation to frog infection status are visualized in Figures S11 and S12. In general, variants in the *Bd*-infected frog subsets showed higher values of nucleotide diversity and Tajima's D. The mean Tajima's D in *Bd*-infected frogs was 0.59 ($SD = 0.723$), while the value was slightly lower in the uninfected

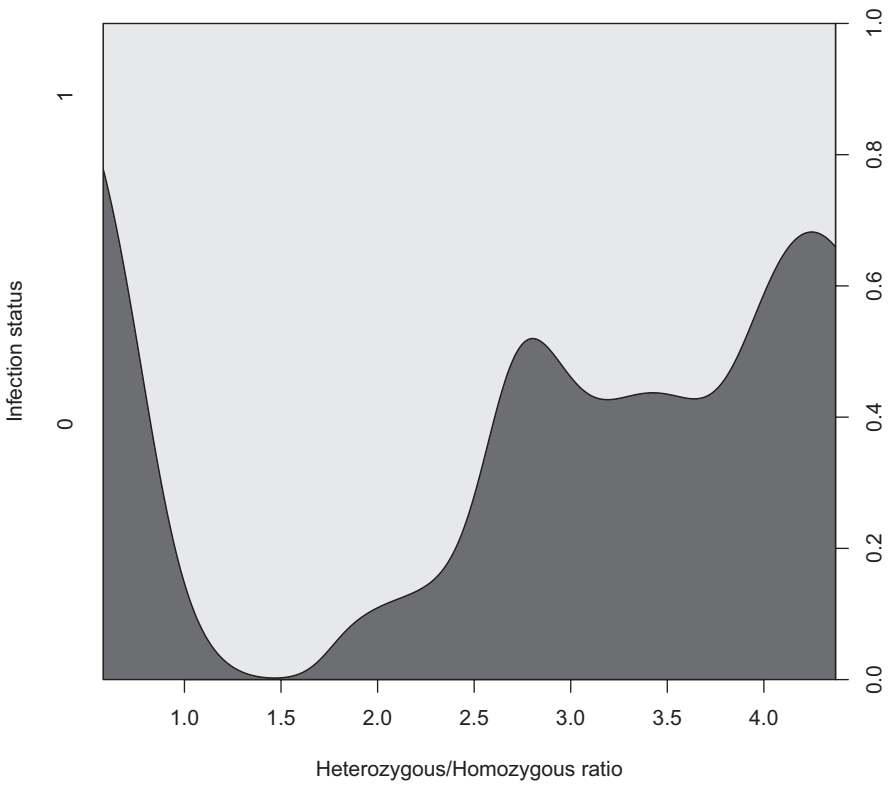

FIGURE 3 Conditional density of *Batrachochytrium dendrobatidis* (*Bd*) infection status related to individual heterozygosity. Dark grey colour distribution represents the probability of frog being uninfected (0), while light grey colour represents *Bd*-infected (1). Probability is illustrated in the right *y*-axis

individuals (mean = 0.525, *SD* = 0.745). The distribution of Tajima's D values differed for these two groups of frogs (Mann–Whitney–Wilcoxon test $W = 1{,}858{,}827$, $p = .0178$).

Distance matrices and genetic relationships among frogs used to identify clustering patterns mainly regarding animal infection status are shown in Figure S13 for scatter plots representing first dimensions of the MDS analyses of the IBS distance matrix, and in Figure S14 for heatmaps representing IBD distance matrix. We found no clear pattern of genetic differentiation among the sequenced 77 coqui frogs either using *data set 1* (Figures S13A and S14A) and *5* (Figures S13B and S14B), or using the subset of these data sets with only variants that deviated from HWE with loss of heterozygosity (Figures S13C,D and S14C,D). We also assessed population differentiation by analysing the molecular variance between initial infection status. We detected that most of the variance in the genetic distance matrix arose from samples within the same infection category (sigma and phi statistics zero or slightly negative, see Table S3 for the components of variation). These results pointed to random mating among *Bd*-infected and uninfected frogs. Likewise, when we estimated population differentiation and admixture, we found that the 77 frogs belong to the same ancestral population (Figures S15 and S16). Our comparison between the two demographic models supported the bottleneck model as the best-fitting model for this coqui population. From the bottleneck run with smaller likelihood difference, the estimates of demographic parameters of this coqui population showed that the ancestral population size (N_{ANC}) was 592,336 (values for the 100 analysis runs ranged from 592,336 to 2,623,435), while our current population size estimate (N_{CUR}) was 141 (values for the 100 analysis runs ranged from 141 to 61,493, see Table S4). Time to the bottleneck (T_{BOT}) was 26 generations (values for the 100 analysis runs ranged from 21 to 1029). Nevertheless, the bottleneck population size was greater than the current effective population size estimation ($N_{BOT} = 2954$; values for the 100 analysis runs ranged from 453 to 10,761) indicating that this population is probably still in decline (Figure 2).

We described the relationships among pathogen–microbiome–hosts in analytical frameworks (Figures 4, S17). The multivariate statistical analysis results from the structural equation models are shown in Table S5 for the *initial* data and Table S6 for the *experimental* data. We confirmed hypothesized relationships such as the correlation of climatic seasons with host body condition and microbiome diversity upon frog capture. In the warm-wet season frogs were in better condition with a relatively low skin microbiome diversity index (Figure 4; Table S5). At the same time, season had indirect effects on the abundance of *Acinetobacter rhizosphaerae* through both animal body condition and microbiome diversity. The abundance of this skin bacterium was also correlated with *Bd* infection status and frog heterozygosity (Figure 4; Table S5). We found a potential offsetting effect of frog heterozygosity on *Bd* infection status and the abundance of *A. rhizosphaerae* in the skin. While high levels of heterozygosity were correlated with a higher abundance of *A. rhizosphaerae* in the frog skin, we found a positive relationship between *Bd*-infected frogs and the abundance of this bacterium. On the other hand, for the *experimental* data, the treatment category was the main cause of the change in both microbiome diversity and *Bd* load, the latter variable, as expected, being negative correlated with frog recovery (Figure S17 and Table S6).

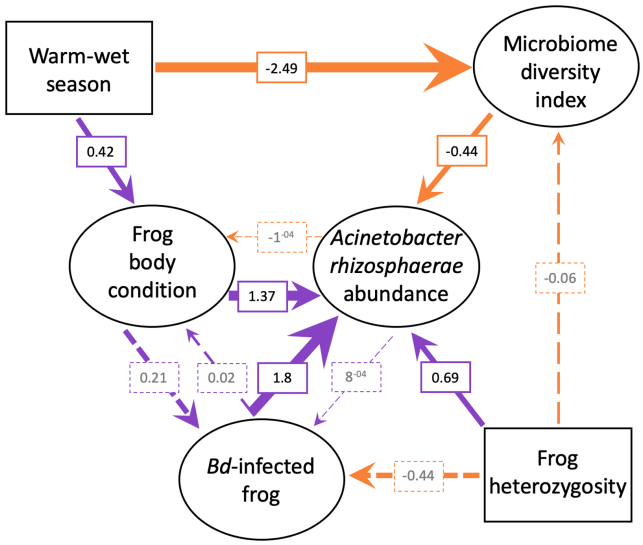

FIGURE 4 Direct acyclic graph of symbiotic interactions representing the structural equation model of the *initial* data set. Exogenous variables are represented in squares and endogenous variables in circles. Correlations between variables are illustrated with arrows and estimated coefficients are included in the boxes. Arrow colour represents the direction of the relationship (positive = violet and negative = orange), the width shows the effect size (larger arrows describe higher magnitude effects), and the type of line illustrates the significance of the relationship in the structural equation models (solid lines = $p < .05$ and dashed lines = $p = .05$) [Colour figure can be viewed at wileyonlinelibrary.com]

4 | DISCUSSION

Symbiotic interactions can determine the evolution of host species, influencing genetic variation through, for instance, selection processes and changes in demography. We generated genome-wide data of an amphibian species to find evidence of symbionts' evolutionary pressures. The trifecta in the evolutionary race of our study consisted of a globally distributed batrachochytrid pathogen (*Bd*), an antifungal bacterium facultative resident of the amphibian skin (*Acinetobacter rhizosphaerae*) and an anuran under *Bd* infection cycles (*Eleutherodactylus coqui*). We found that our focal frog population had severely decreased its effective population size (N_e) plausibly due to *Bd* emergence. At the same time, we uncovered frog genetic variation and potential heterozygote advantage to recruit *A. rhizosphaerae* and fight *Bd* infections.

Since the detection of the first amphibian die-offs due to *Bd* (Berger et al., 1998; Bosch et al., 2001), hundreds of population declines have been reported (Fisher & Garner, 2020; Scheele et al., 2019). Despite the importance of these losses for the declining species, their communities and ecosystems (Zipkin et al., 2020), the evolutionary consequences of population size changes are rarely evaluated. Reductions in N_e exacerbate the intensity of genetic drift and impact adaptation processes (Charlesworth, 2009; Papkou et al., 2016). Declines in frog abundance at the locality of this study, Palo Colorado Forest at El Yunque, have been documented since 1989 (Burrowes et al., 2004). These losses were related to the synergic effects between *Bd* infection and droughts, potentially exacerbated by hurricane Hugo (Woolbright, 1991). We uncovered a severe population bottleneck in this studied coquí frog population, with a drastic collapse in several orders of magnitude of the contemporary N_e. As a consequence, our findings suggest that the declines over the last 30 years have impacted the evolutionary trajectory of this population, weakening the effectiveness of selection processes through the reduction of N_e. Although in situ monitoring showed patterns of population recovery (Longo & Burrowes, 2010), our findings point to stochastic processes limiting adaptation. Also, interactions with environmental conditions can impose additional costs delaying evolutionary processes. Potentially adapted and nonadapted frogs survive *Bd* infection during the warm-wet season (Longo et al., 2010). Our results suggested random mating in the population, supporting our hypothesis that both adapted and nonadapted frogs can theoretically produce offspring and are contributing to recruitment in the population. In other words, frogs possibly reproduce without assortative mating due to infection status, which might be driven by low infection intensities and high prevalence in the population. Hence, alleles under selection might have not been fixed yet or presented at high frequencies in the population. In the same mountainous system, coqui population recoveries at higher elevations and an absence of declines at lower elevations have been observed (Burrowes et al., 2004; Longo & Burrowes, 2010). Additional comparisons of host genetics in localities with high variation in environmental conditions and/or different responses to *Bd* infection could better unravel this evolutionary process of co-adaptation (Savage et al., 2015).

Increased genetic diversity can lessen infectious disease risk in a population (DeCandia et al., 2018; King & Lively, 2012). For example, genetically depauperate populations have been compared to monocultures in agriculture, where higher infection prevalence and transmission occur across similar host genotypes (King & Lively, 2012). During an experimental evolution study, a chytrid fungal parasite (*Rhizophydium megarrhizum* Skuja, 1956) caused higher intensity infections in monoclonal hosts, highlighting that genetic diversity can limit the increase of the parasite fitness (Agha et al., 2018). Consistent with these results, we detected a relatively lower nucleotide diversity in the *Bd*-infected frogs. Other amphibian populations impacted by *Bd* have shown dramatic decreases in genetic diversity, such as the contemporary Panamanian populations of *Atelopus varius* (Lichtenstein & Martens, 1856) (Byrne et al., 2021). This species has been on the brink of extinction, but population recoveries suggest the evolution of host defence mechanisms (Voyles et al., 2018). Neutral genetic diversity, which lacks adaptive diversity information, sometimes fails to identify associations with population health and future disease risk (DeCandia et al., 2018; Teixeira & Huber, 2021). Our nucleotide-based metrics were computed from variants identified through a restriction enzyme sequencing method and included neutral markers, so even with an overall decrease of the genetic diversity, *Bd*-infected coquí frogs can still harbour variation in functional genomic locations for adaptation to *Bd* infection. Targeting defence (epi)genetic regions including the components of the MHC (Fu & Waldman, 2017; Richmond et al., 2009) and genes involved

in mechanisms that impede pathogen growth, such as nutritional immune-related genes (Torres-Sánchez et al., 2022), could further improve our understanding of population dynamics, especially to generate better predictions of its evolutionary trajectory.

In diploid organisms, theoretical frameworks based on Fisher's geometric model predict that adaptive mutations increase the fitness of heterozygotes, a phenomenon known as heterozygote advantage (Fisher, 1930; Sellis et al., 2011). Heterozygosity correlations with fitness-related traits have been explored to investigate the evolutionary consequences of genetic diversity at the individual level (Chapman et al., 2009; Turelli, 1983). Genome-wide heterozygosity is interpreted under the "general effect" hypothesis: loci through the whole genome covary, being in identity disequilibrium (David, 1998). Our study revealed that coquí frogs with low genome-wide heterozygosity were more likely to be *Bd*-infected. A genome-wide analysis of another anuran, *Litoria verreauxii alpina* (Fry, 1915), also shows that greater individual heterozygosity was associated with a reduced probability of *Bd* infection (Banks et al., 2020). Other studies have found the opposite heterozygosity–*Bd* infection relationship in other amphibian species when analysing the genetic diversity of a small number of genetic markers, 11 and seven nuclear microsatellites, respectively (Addis et al., 2015; Horner et al., 2017), which might not be representative of their whole genomes. Immunogenetic research focusing on the class II MHC has presented both relationships, where heterozygous individuals through balancing selection and homozygous individuals with alleles under strong directional selection have a low *Bd* infection risk (Belasen et al., 2022; Fu & Waldman, 2017; Kosch et al., 2016; Savage & Zamudio, 2011). In our evolutionary scenario, *Bd* infection status might not be the best proxy of frog fitness, because infected coqui frogs can survive even during the cool-dry season (Longo et al., 2010). Alternatively, through our structural equation model, we found that the abundance of the putative defence symbiont *A. rhizosphaerae* was positively correlated with frog heterozygosity. We propose this variable as a more adequate fitness trait, which should be further examined to assess the potential protection mechanism through, for instance, challenge trials. Interestingly, in this multipartite interaction, we discovered a potential offsetting effect of this heterozygosity–fitness correlation (Laughlin & Grace, 2019), which might reflect different ecological and evolutionary processes in the interaction among the three species (Hopkins et al., 2017). Heterozygosity ratios tended to be higher in uninfected frogs and were also correlated with higher abundance of the candidate beneficial bacterium. At the same time, *Bd*-infected frogs carried a high abundance of *A. rhizosphaerae*. Different studies have shown that *A. rhizosphaerae* can inhibit but also can enhance *Bd* growth or even has no detectable effect (Muletz-Wolz et al., 2017; Woodhams et al., 2015). We hypothesized that the interactions among *Bd*, *A. rhizosphaerae* and *E. coqui* reflect the dynamics of the infection process. At first, during *Bd* colonization of amphibian skin, a positive association of the pathogen and the candidate antifungal bacterium might occur, plausibly reflecting attraction mediated through secondary metabolites. The increase of *A. rhizosphaerae* in the amphibian skin could contribute to fighting *Bd* infection. As a consequence, uninfected frogs that have removed the pathogen could present a high abundance of *A. rhizosphaerae*, and potentially frogs with higher heterozygosity levels could maintain this candidate beneficial bacterium to avoid reinfection by *Bd*, which is consistently present in this coqui frog population. Amphibian skin is a unique ecosystem with complex communities of microorganisms, whose diversity has been globally related to the host environmental conditions (Kueneman et al., 2019). We expected to find a strong signal between frog individual heterozygosity and the microbiome diversity index, yet we failed to detect this correlation. The role of the amphibian host in shaping the diversity and structure of their skin microbiome could be indirect through the interaction with specific members (Bletz et al., 2017). This scenario has been defined as "ecosystem on a leash" (Foster et al., 2017). We hypothesize that coqui frogs, their candidate beneficial bacterium and their pathogen are under this eco-evolutionary model of interactions, which could improve host health by preserving skin microbiome functional diversity (Longo, 2022). Considering that coqui frogs are invasive in many parts of the world, independent colonization events could provide the ideal system to further examine eco-evolutionary interactions using modelling, field observations and experimental approaches.

Symbiotic interactions are ubiquitous, impacting the ecology and evolution of their host species. To better understand the species dynamics, multipartite interactions need to be examined more often, especially when symbionts use a common resource. Here, we defined an interaction model that can be theoretically evaluated to gain further insights into the evolutionary trajectories of coquí frogs. Future research directions should assess the intergenerational transmission, measure the heritability of the symbionts, and, ultimately, characterize correlations between symbiont genotypes and host genetic diversity (Parker et al., 2017). Integrating the genetic data of all the partners will enhance our understanding of symbiotic systems. Regarding the global amphibian decline crisis, knowledge of codiversification dynamics is essential to improve the efficiency of conservation actions, especially those considering bioaugmentation strategies (Bletz et al., 2013).

AUTHOR CONTRIBUTIONS

M.T.-S. and A.V.L. designed the research; A.V.L. performed DNA extractions; M.T.-S. analysed the data and wrote the original draft; both authors reviewed and approved the final manuscript.

ACKNOWLEDGEMENTS

We thank HiPerGator at the University of Florida for technical support and computational resources. We express our gratitude to the Subject Editor and Reviewers for their comments, which helped us to improve the manuscript. We also thank Iván de la Hera, Alex Llanos-Garrido and George Glen for valuable feedback. This work was supported by NSF Grants IOS-2011278 and IOS-1310036, UF CLAS Research Office, and the Department of Biology startup funds.

CONFLICT OF INTEREST

The authors declare no competing interest.

OPEN RESEARCH BADGES

This article has earned an Open Data badge for making publicly available the digitally-shareable data necessary to reproduce the reported results. The data is available at https://github.com/TorresSanchezM/coqui_GBS.

DATA AVAILABILITY STATEMENT

The generated genomic data have been deposited in the Sequence Read Archive, (BioProject accession no. PRJNA833081). Traits and variables for each frog are included in Appendix S1. The variant calling format file containing the initial genomic data set or *data set 1* can be found in Appendix S2. Complete code for the analyses including parameter specifications can be found in Appendix S3. The data are also available at https://github.com/TorresSanchezM/coqui_GBS.

ORCID

María Torres-Sánchez https://orcid.org/0000-0001-8484-9279
Ana V. Longo https://orcid.org/0000-0002-5112-1246

REFERENCES

Addis, B. R., Lowe, W. H., Hossack, B. R., & Allendorf, F. W. (2015). Population genetic structure and disease in montane boreal toads: More heterozygous individuals are more likely to be infected with amphibian chytrid. *Conservation Genetics*, *16*, 833–844. https://doi.org/10.1007/s10592-015-0704-6

Agha, R., Gross, A., Rohrlack, T., & Wolinska, J. (2018). Adaptation of a chytrid parasite to its cyanobacterial host is hampered by host intraspecific diversity. *Frontiers in Microbiology*, *9*, 921. https://doi.org/10.3389/fmicb.2018.00921

Alexander, D. H., Novembre, J., & Lange, K. (2009). Fast model-based estimation of ancestry in unrelated individuals. *Genome Research*, *19*(9), 1655–1664. https://doi.org/10.1101/gr.094052.109

Andersen, S. B., Gerritsma, S., Yusah, K. M., Mayntz, D., Hywel-Jones, N. L., Billen, J., Boomsma, J. J., & Hughes, D. P. (2009). The life of a dead ant: The expression of an adaptive extended phenotype. *The American Naturalist*, *174*, 424–433. https://doi.org/10.1086/603640

Banks, S. C., Scheele, B. C., Macris, A., Hunter, D., Jack, C., & Fraser, C. I. (2020). Chytrid fungus infection in alpine tree frogs is associated with individual heterozygosity and population isolation but not population-genetic diversity. *Frontiers of Biogeography*, *12*, e43875. https://doi.org/10.21425/f5fbg43875

Bates, K. A., Clare, F. C., O'Hanlon, S., Bosch, J., Brookes, L., Hopkins, K., McLaughlin, E., Daniel, O., Garner, T. W. J., Fisher, M. C., & Harrison, X. A. (2018). Amphibian chytridiomycosis outbreak dynamics are linked with host skin bacterial community structure. *Nature Communications*, *9*, 693. https://doi.org/10.1038/s41467-018-02967-w

Belasen, A., Amses, K., Clemons, R., Becker, G., Toledo, F., & James, T. (2022). Habitat fragmentation in the Brazilian Atlantic Forest is associated with erosion of frog immunogenetic diversity and increased fungal infections. *Immunogenetics*, *74*, 431–441. https://doi.org/10.1007/s00251-022-01252-x

Berger, L., Speare, R., Daszak, P., Green, D. E., Cunningham, A. A., Goggin, C. L., Slocombe, R., Ragan, M. A., Hyatt, A. D., McDonald, K., Hines, H. B., Lips, K. R., Marantelli, G., & Parkes, H. (1998). Chytridiomycosis causes amphibian mortality associated with population declines in the rain forests of Australia and Central America. *Proceedings of the National Academy of Sciences of the United States of America*, *95*, 9031–9036. https://doi.org/10.1073/pnas.95.15.9031

Bletz, M. C., Loudon, A. H., Becker, M. H., Bell, S. C., Woodhams, D. C., Minbiole, K. P. C., & Harris, R. N. (2013). Mitigating amphibian chytridiomycosis with bioaugmentation: Characteristics of effective probiotics and strategies for their selection and use. *Ecology Letters*, *16*, 807–820. https://doi.org/10.1111/ele.12099

Bletz, M. C., Perl, R. G. B., Bobowski, B. T. C., Japke, L. M., Tebbe, C. C., Dohrmann, A. B., Bhuju, S., Geffers, R., Jarek, M., & Vences, M. (2017). Amphibian skin microbiota exhibits temporal variation in community structure but stability of predicted Bd-inhibitory function. *The ISME Journal*, *11*, 1521–1534. https://doi.org/10.1038/ismej.2017.41

Bosch, J., Martínez-Solano, I., & García-París, M. (2001). Evidence of a chytrid fungus infection involved in the decline of the common midwife toad (*Alytes obstetricans*) in protected areas of Central Spain. *Biological Conservation*, *97*, 331–337. https://doi.org/10.1016/S0006-3207(00)00132-4

Bradbury, P. J., Zhang, Z., Kroon, D. E., Casstevens, T. M., Ramdoss, Y., & Buckler, E. S. (2007). TASSEL: Software for association mapping of complex traits in diverse samples. *Bioinformatics*, *23*, 2633–2635. https://doi.org/10.1093/bioinformatics/btm308

Brannelly, L. A., McCallum, H. I., Grogan, L. F., Briggs, C. J., Ribas, M. P., Hollanders, M., Sasso, T., Familiar López, M., Newell, D. A., & Kilpatrick, A. M. (2021). Mechanisms underlying host persistence following amphibian disease emergence determine appropriate management strategies. *Ecology Letters*, *24*, 130–148. https://doi.org/10.1111/ele.13621

Briggs, C. J., Knapp, R. A., & Vredenburg, V. T. (2010). Enzootic and epizootic dynamics of the chytrid fungal pathogen of amphibians. *Proceedings of the National Academy of Sciences of the United States of America*, *107*, 9695–9700. https://doi.org/10.1073/pnas.0912886107

Burrowes, P. A., Joglar, R. L., & Green, D. E. (2004). Potential causes for amphibian declines in Puerto Rico. *Herpetologica*, *60*, 141–154. https://doi.org/10.1655/03-50

Burrowes, P. A., Martes, M. C., Torres-Ríos, M., & Longo, A. V. (2017). Arboreality predicts Batrachochytrium dendrobatidis infection level in tropical direct-developing frogs. *Journal of Natural History*, *51*, 643–656. https://doi.org/10.1080/00222933.2017.1297504

Byrne, A. Q., Richards-Zawacki, C. L., Voyles, J., Bi, K., Ibáñez, R., & Rosenblum, E. B. (2021). Whole exome sequencing identifies the potential for genetic rescue in iconic and critically endangered Panamanian harlequin frogs. *Global Change Biology*, *27*, 50–70. https://doi.org/10.1111/gcb.15405

Caporaso, J. G., Kuczynski, J., Stombaugh, J., Bittinger, K., Bushman, F. D., Costello, E. K., Fierer, N., Peña, A. G., Goodrich, J. K., Gordon, J. I., Huttley, G. A., Kelley, S. T., Knights, D., Koenig, J. E., Ley, R. E., Lozupone, C. A., McDonald, D., Muegge, B. D., Pirrung, M., … Knight, R. (2010). QIIME allows analysis of high-throughput community sequencing data. *Nature Methods*, *7*, 335–336. https://doi.org/10.1038/nmeth.f.303

Chapman, J. R., Nakagawa, S., Coltman, D. W., Slate, J., & Sheldon, B. C. (2009). A quantitative review of heterozygosity-fitness correlations in animal populations. *Molecular Ecology*, *18*, 2746–2765. https://doi.org/10.1111/j.1365-294X.2009.04247.x

Charlesworth, B. (2009). Effective population size and patterns of molecular evolution and variation. *Nature Reviews. Genetics*, *10*, 195–205. https://doi.org/10.1038/nrg2526

Crawford, A. J. (2003). Relative rates of nucleotide substitution in frogs. *Journal of Molecular Evolution*, *57*, 636–641. https://doi.org/10.1007/s00239-003-2513-7

Danecek, P., Auton, A., Abecasis, G., Albers, C. A., Banks, E., DePristo, M. A., Handsaker, R. E., Lunter, G., Marth, G. T., Sherry, S. T., McVean, G., Durbin, R., & 1000 Genomes Project Analysis Group.

(2011). The variant call format and VCFtools. *Bioinformatics*, *27*(15), 2156–2158. https://doi.org/10.1093/bioinformatics/btr330

David, P. (1998). Heterozygosity-fitness correlations: New perspectives on old problems. *Heredity*, *80*, 531–537. https://doi.org/10.1046/j.1365-2540.1998.00393.x

DeCandia, A. L., Dobson, A. P., & vonHoldt, B. M. (2018). Toward an integrative molecular approach to wildlife disease. *Conservation Biology*, *32*, 798–807. https://doi.org/10.1111/cobi.13083

Elshire, R. J., Glaubitz, J. C., Sun, Q., Poland, J. A., Kawamoto, K., Buckler, E. S., & Mitchell, S. E. (2011). A robust, simple genotyping-by-sequencing (GBS) approach for high diversity species. *PLoS One*, *6*, e19379. https://doi.org/10.1371/journal.pone.0019379

Excoffier, L., Dupanloup, I., Huerta-Sánchez, E., Sousa, V. C., & Foll, M. (2013). Robust demographic inference from genomic and SNP data. *PLoS Genetics*, *9*, e1003905. https://doi.org/10.1371/journal.pgen.1003905

Fisher, M. C., & Garner, T. W. J. (2020). Chytrid fungi and global amphibian declines. *Nature Reviews. Microbiology*, *18*, 332–343. https://doi.org/10.1038/s41579-020-0335-x

Fisher, M. C., Gurr, S. J., Cuomo, C. A., Blehert, D. S., Jin, H., Stukenbrock, E. H., Stajich, J. E., Kahmann, R., Boone, C., Denning, D. W., Gow, N. A. R., Klein, B. S., Kronstad, J. W., Sheppard, D. C., Taylor, J. W., Wright, G. D., Heitman, J., Casadevall, A., & Cowen, L. E. (2020). Threats posed by the fungal kingdom to humans, wildlife, and agriculture. *MBio*, *11*, e00449–20. https://doi.org/10.1128/mBio.00449-20

Fisher, M. C., Henk, D. A., Briggs, C. J., Brownstein, J. S., Madoff, L. C., McCraw, S. L., & Gurr, S. J. (2012). Emerging fungal threats to animal, plant and ecosystem health. *Nature*, *484*, 186–194. https://doi.org/10.1038/nature10947

Fisher, R. A. (1930). *The genetical theory of natural selection*. Clarendon Press. https://doi.org/10.5962/bhl.title.27468

Fisher, R. M., Henry, L. M., Cornwallis, C. K., Kiers, E. T., & West, S. A. (2017). The evolution of host-symbiont dependence. *Nature Communications*, *8*, 15973. https://doi.org/10.1038/ncomms15973

Foster, K. R., Schluter, J., Coyte, K. Z., & Rakoff-Nahoum, S. (2017). The evolution of the host microbiome as an ecosystem on a leash. *Nature*, *548*, 43–51. https://doi.org/10.1038/nature23292

Fu, M., & Waldman, B. (2017). Major histocompatibility complex variation and the evolution of resistance to amphibian chytridiomycosis. *Immunogenetics*, *69*, 529–536. https://doi.org/10.1007/s00251-017-1008-4

Glaubitz, J. C., Casstevens, T. M., Lu, F., Harriman, J., Elshire, R. J., Sun, Q., & Buckler, E. S. (2014). TASSEL-GBS: A high capacity genotyping by sequencing analysis pipeline. *PLoS One*, *9*, e90346. https://doi.org/10.1371/journal.pone.0090346

Greenspan, S. E., Lambertini, C., Carvalho, T., James, T. Y., Toledo, L. F., Haddad, C. F. B., & Becker, C. G. (2018). Hybrids of amphibian chytrid show high virulence in native hosts. *Scientific Reports*, *8*, 9600. https://doi.org/10.1038/s41598-018-27828-w

Hayward, A., Poulin, R., & Nakagawa, S. (2021). A broadscale analysis of host-symbiont cophylogeny reveals the drivers of phylogenetic congruence. *Ecology Letters*, *24*, 1681–1696. https://doi.org/10.1111/ele.13757

Hopkins, S. R., Wojdak, J. M., & Belden, L. K. (2017). Defensive symbionts mediate host–parasite interactions at multiple scales. *Trends in Parasitology*, *33*, 53–64. https://doi.org/10.1016/j.pt.2016.10.003

Horner, A. A., Hoffman, E. A., Tye, M. R., Hether, T. D., & Savage, A. E. (2017). Cryptic chytridiomycosis linked to climate and genetic variation in amphibian populations of the southeastern United States. *PLoS One*, *12*, e0175843. https://doi.org/10.1371/journal.pone.0175843

Hurst, G. D. D. (2017). Extended genomes: Symbiosis and evolution. *Interface Focus*, *7*, 20170001. https://doi.org/10.1098/rsfs.2017.0001

Jani, A. J., Knapp, R. A., & Briggs, C. J. (2017). Epidemic and endemic pathogen dynamics correspond to distinct host population microbiomes at a landscape scale. *Proceedings of the Royal Society B: Biological Sciences*, *284*, 20170944. https://doi.org/10.1098/rspb.2017.0944

King, K. C., & Lively, C. M. (2012). Does genetic diversity limit disease spread in natural host populations. *Heredity*, *109*, 199–203. https://doi.org/10.1038/hdy.2012.33

Kosch, T. A., Bataille, A., Didinger, C., Eimes, J. A., Rodríguez-Brenes, S., Ryan, M. J., & Waldman, B. (2016). Major histocompatibility complex selection dynamics in pathogen-infected túngara frog (*Physalaemus pustulosus*) populations. *Biology Letters*, *12*(8), 20160345. https://doi.org/10.1098/rsbl.2016.0345

Kueneman, J. G., Bletz, M. C., McKenzie, V. J., Becker, C. G., Joseph, M. B., Abarca, J. G., Archer, H., Arellano, A. L., Bataille, A., Becker, M., Belden, L. K., Crottini, A., Geffers, R., Haddad, C. F. B., Harris, R. N., Holden, W. M., Hughey, M., Jarek, M., Kearns, P. J., … Vences, M. (2019). Community richness of amphibian skin bacteria correlates with bioclimate at the global scale. *Nature Ecology and Evolution.*, *3*, 381–389. https://doi.org/10.1038/s41559-019-0798-1

Langhammer, P. F., Burrowes, P. A., Lips, K. R., Bryant, A. B., & Collins, J. P. (2014). Susceptibility to the amphibian chytrid fungus varies with ontogeny in the direct-developing frog, Eleutherodactylus Coqui. *Journal of Wildlife Diseases*, *50*, 438–446. https://doi.org/10.7589/2013-10-268

Laughlin, D., & Grace, J. (2019). Discoveries and novel insights in ecology using structural equation modeling. *Ideas in Ecology and Evolution*, *12*, 28–34. https://doi.org/10.24908/iee.2019.12.5.c

Lefcheck, J. S. (2016). piecewiseSEM: Piecewise structural equation modelling in r for ecology, evolution, and systematics. *Methods in Ecology and Evolution*, *7*, 573–579. https://doi.org/10.1111/2041-210X.12512

Lepais, O., & Weir, J. T. (2014). SimRAD: An R package for simulation-based prediction of the number of loci expected in RADseq and similar genotyping by sequencing approaches. *Molecular Ecology Resources*, *14*, 1314–1321. https://doi.org/10.1111/1755-0998.12273

Longcore, J. E., Pessier, A. P., & Nichols, D. K. (1999). *Batrachochytrium dendrobatidis* gen. Et sp. nov., a chytrid pathogenic to amphibians. *Mycologia*, *91*, 219–227. https://doi.org/10.2307/3761366

Longo, A. V. (2022). Metabarcoding approaches in amphibian disease ecology: Disentangling the functional contributions of skin bacteria on disease outcome. *Integrative and Comparative Biology*, *62*(2), 252–261. https://doi.org/10.1093/icb/icac062

Longo, A. V., & Burrowes, P. A. (2010). Persistence with chytridiomycosis does not assure survival of direct-developing frogs. *EcoHealth*, *7*, 185–195. https://doi.org/10.1007/s10393-010-0327-9

Longo, A. V., Burrowes, P. A., & Joglar, R. L. (2010). Seasonality of Batrachochytrium dendrobatidis infection in direct-developing frogs suggests a mechanism for persistence. *Diseases of Aquatic Organisms*, *92*, 253–260. https://doi.org/10.3354/dao02054

Longo, A. V., & Zamudio, K. R. (2017). Environmental fluctuations and host skin bacteria shift survival advantage between frogs and their fungal pathogen. *The ISME Journal*, *11*, 349–361. https://doi.org/10.1038/ismej.2016.138

Margulis, L. (1998). *Symbiotic planet: A new look at evolution*. Basic Books. https://doi.org/10.5860/choice.36-6268

McFall-Ngai, M., Hadfield, M. G., Bosch, T. C. G., Carey, H. V., Domazet-Lošo, T., Douglas, A. E., Dubilier, N., Eberl, G., Fukami, T., Gilbert, S. F., Hentschel, U., King, N., Kjelleberg, S., Knoll, A. H., Kremer, N., Mazmanian, S. K., Metcalf, J. L., Nealson, K., Pierce, N. E., … Wernegreen, J. J. (2013). Animals in a bacterial world, a new imperative for the life sciences. *Proceedings of the National Academy of Sciences of the United States of America*, *110*, 3229–3236. https://doi.org/10.1073/pnas.1218525110

Muletz-Wolz, C. R., Almario, J. G., Barnett, S. E., DiRenzo, G. V., Martel, A., Pasmans, F., Zamudio, K. R., Toledo, L. F., & Lips, K. R. (2017).

Inhibition of fungal pathogens across genotypes and temperatures by amphibian skin bacteria. *Frontiers in Microbiology*, *8*(AUG), 1–10. https://doi.org/10.3389/fmicb.2017.01551

Naranjo-Ortiz, M. A., & Gabaldón, T. (2019a). Fungal evolution: Diversity, taxonomy and phylogeny of the fungi. *Biological Reviews*, *94*, 2101–2137. https://doi.org/10.1111/brv.12550

Naranjo-Ortiz, M. A., & Gabaldón, T. (2019b). Fungal evolution: Major ecological adaptations and evolutionary transitions. *Biological Reviews*, *94*, 1443–1476. https://doi.org/10.1111/brv.12510

Olson, D. H., Ronnenberg, K. L., Glidden, C. K., Christiansen, K. R., & Blaustein, A. R. (2021). Global patterns of the fungal pathogen *Batrachochytrium dendrobatidis* support conservation urgency. *Frontiers in Veterinary Science*, *8*, 685877. https://doi.org/10.3389/fvets.2021.685877

Papkou, A., Gokhale, C. S., Traulsen, A., & Schulenburg, H. (2016). Host–parasite coevolution: Why changing population size matters. *Zoology*, *119*, 330–338. https://doi.org/10.1016/j.zool.2016.02.001

Paradis, E. (2010). Pegas: An R package for population genetics with an integrated-modular approach. *Bioinformatics*, *26*, 419–420. https://doi.org/10.1093/bioinformatics/btp696

Parker, B. J., Hrček, J., McLean, A. H. C., & Godfray, H. C. J. (2017). Genotype specificity among hosts, pathogens, and beneficial microbes influences the strength of symbiont-mediated protection. *Evolution*, *71*, 1222–1231. https://doi.org/10.1111/evo.13216

Purcell, S., Neale, B., Todd-Brown, K., Thomas, L., Ferreira, M. A. R., Bender, D., Maller, J., Sklar, P., de Bakker, P. I., Daly, M. J., & Sham, P. C. (2007). PLINK: A tool set for whole-genome association and population-based linkage analyses. *The American Journal of Human Genetics*, *81*(3), 559–575. https://doi.org/10.1086/519795

R Core Team. (2019). *R: A language and environment for statistical computing*. R Foundation for Statistical Computing.

Richmond, J. Q., Savage, A. E., Zamudio, K. R., & Rosenblum, E. B. (2009). Toward immunogenetic studies of amphibian chytridiomycosis: Linking innate and acquired immunity. *Bioscience*, *59*, 311–320. https://doi.org/10.1525/bio.2009.59.4.9

Savage, A. E., Becker, C. G., & Zamudio, K. R. (2015). Linking genetic and environmental factors in amphibian disease risk. *Evolutionary Applications*, *8*, 560–572. https://doi.org/10.1111/eva.12264

Savage, A. E., & Zamudio, K. R. (2011). MHC genotypes associate with resistance to a frog-killing fungus. *Proceedings of the National Academy of Sciences of the United States of America*, *108*, 16705–16710. https://doi.org/10.1073/pnas.1106893108

Scheele, B. C., Pasmans, F., Skerratt, L. F., Berger, L., Martel, A., Beukema, W., Acevedo, A. A., Burrowes, P. A., Carvalho, T., Catenazzi, A., de la Riva, I., Fisher, M. C., Flechas, S. V., Foster, C. N., Frías-Álvarez, P., Garner, T. W. J., Gratwicke, B., Guayasamin, J. M., Hirschfeld, M., … Canessa, S. (2019). Amphibian fungal panzootic causes catastrophic and ongoing loss of biodiversity. *Science*, *363*, 1459–1463. https://doi.org/10.1126/science.aav0379

Schmidt, T. L., Jasper, M., Weeks, A. R., & Hoffmann, A. A. (2021). Unbiased population heterozygosity estimates from genome-wide sequence data. *Methods in Ecology and Evolution*, *12*, 1888–1898. https://doi.org/10.1111/2041-210x.13659

Scholthof, K. B. G. (2007). The disease triangle: Pathogens, the environment and society. *Nature Reviews. Microbiology*, *5*, 152–156. https://doi.org/10.1038/nrmicro1596

Sellis, D., Callahan, B. J., Petrov, D. A., & Messer, P. W. (2011). Heterozygote advantage as a natural consequence of adaptation in diploids. *Proceedings of the National Academy of Sciences of the United States of America*, *108*, 20666–20671. https://doi.org/10.1073/pnas.1114573108

Tajima, F. (1989). Statistical method for testing the neutral mutation hypothesis by DNA polymorphism. *Genetics*, *123*, 585–595. https://doi.org/10.1093/genetics/123.3.585

Teixeira, J. C., & Huber, C. D. (2021). The inflated significance of neutral genetic diversity in conservation genetics. *Proceedings of the National Academy of Sciences of the United States of America*, *118*, e2015096118. https://doi.org/10.1073/pnas.2015096118

Torres-Sánchez, M., Villate, J., McGrath-Blaser, S., & Longo, A. V. (2022). Panzootic chytrid fungus exploits diverse amphibian host environments through plastic infection strategies. *Molecular Ecology*, *31*, 4558–4570. https://doi.org/10.1111/mec.16601

Turelli, M. (1983). Should individual fitness increase with heterozygosity? *Genetics*, *104*, 191–209. https://doi.org/10.1093/genetics/104.1.191

van der Heijden, M. G. A., Martin, F. M., Selosse, M. A., & Sanders, I. R. (2015). Mycorrhizal ecology and evolution: The past, the present, and the future. *The New Phytologist*, *205*, 1406–1423. https://doi.org/10.1111/nph.13288

Vorburger, C., & Perlman, S. J. (2018). The role of defensive symbionts in host–parasite coevolution. *Biological Reviews*, *93*, 1747–1764. https://doi.org/10.1111/brv.12417

Voyles, J., Woodhams, D. C., Saenz, V., Byrne, A. Q., Perez, R., Rios-Sotelo, G., Ryan, M. J., Bletz, M. C., Sobell, F. A., McLetchie, S., Reinert, L., Rosenblum, E. B., Rollins-Smith, L. A., Ibáñez, R., Ray, J. M., Griffith, E. J., Ross, H., & Richards-Zawacki, C. L. (2018). Shifts in disease dynamics in a tropical amphibian assemblage are not due to pathogen attenuation. *Science*, *359*, 1517–1519. https://doi.org/10.1126/science.aao4806

Weatherall, D., Clegg, J., & Kwiatkowski, D. (1997). The role of genomics in studying genetic susceptibility to infectious disease. *Genome Research*, *7*, 967–973. https://doi.org/10.1101/gr.7.10.967

Woodhams, D. C., Alford, R. A., Antwis, R. E., Archer, H., Becker, M. H., Belden, L. K., & McKenzie, V. (2015). Antifungal isolates database of amphibian skin-associated bacteria and function against emerging fungal pathogens. *Ecology*, *96*, 595. https://doi.org/10.1890/14-1837.1

Woolbright, L. L. (1991). The impact of hurricane Hugo on Forest frogs in Puerto Rico. *Biotropica*, *23*, 462. https://doi.org/10.2307/2388267

Zipkin, E. F., DiRenzo, G. V., Ray, J. M., Rossman, S., & Lips, K. R. (2020). Tropical snake diversity collapses after widespread amphibian loss. *Science*, *367*, 814–816. https://doi.org/10.1126/science.aay5733

SUPPORTING INFORMATION

Additional supporting information can be found online in the Supporting Information section at the end of this article.

How to cite this article: Torres-Sánchez, M., & Longo, A. V. (2022). Linking pathogen–microbiome–host interactions to explain amphibian population dynamics. *Molecular Ecology*, *31*, 5784–5794. https://doi.org/10.1111/mec.16701